frontiers in Immunology

ORIGINAL RESEARCH
published: 05 June 2018
doi: 10.3389/fimmu.2018.01290

T Cell Receptor–Major Histocompatibility Complex Interaction Strength Defines Trafficking and CD103$^+$ Memory Status of CD8 T Cells in the Brain

*Anna Sanecka[1†], Nagisa Yoshida[1], Elizabeth Motunrayo Kolawole[2], Harshil Patel[3], Brian D. Evavold[3] and Eva-Maria Frickel[1]**

[1] Host-Toxoplasma Interaction Laboratory, The Francis Crick Institute, London, United Kingdom, [2] Division of Microbiology and Immunology, Department of Pathology, University of Utah, Salt Lake City, UT, United States, [3] Bioinformatics and Biostatistics, The Francis Crick Institute, London, United Kingdom

OPEN ACCESS

Edited by:
Surojit Sarkar,
University of Washington,
United States

Reviewed by:
Brian S. Sheridan,
Stony Brook University,
United States
Julia Emiley Prier,
University of Melbourne,
Australia

***Correspondence:**
Eva-Maria Frickel
eva.frickel@crick.ac.uk

†Present address:
Anna Sanecka,
Department of Immunology,
Faculty of Biochemistry, Biophysics,
and Biotechnology, Jagiellonian
University, Krakow, Poland

Specialty section:
This article was submitted to
Immunological Memory,
a section of the journal
Frontiers in Immunology

Received: 09 February 2018
Accepted: 23 May 2018
Published: 05 June 2018

Citation:
Sanecka A, Yoshida N, Kolawole EM,
Patel H, Evavold BD and Frickel E-M
(2018) T Cell Receptor–Major
Histocompatibility Complex
Interaction Strength Defines
Trafficking and CD103$^+$ Memory
Status of CD8 T Cells in the Brain.
Front. Immunol. 9:1290.
doi: 10.3389/fimmu.2018.01290

T cell receptor–major histocompatibility complex (TCR–MHC) affinities span a wide range in a polyclonal T cell response, yet it is undefined how affinity shapes long-term properties of CD8 T cells during chronic infection with persistent antigen. Here, we investigate how the affinity of the TCR–MHC interaction shapes the phenotype of memory CD8 T cells in the chronically *Toxoplasma gondii*-infected brain. We employed CD8 T cells from three lines of transnuclear (TN) mice that harbor in their endogenous loci different T cell receptors specific for the same *Toxoplasma* antigenic epitope ROP7. The three TN CD8 T cell clones span a wide range of affinities to MHCI–ROP7. These three CD8 T cell clones have a distinct and fixed hierarchy in terms of effector function in response to the antigen measured as proliferation capacity, trafficking, T cell maintenance, and memory formation. In particular, the T cell clone of lowest affinity does not home to the brain. The two higher affinity T cell clones show differences in establishing resident-like memory populations (CD103$^+$) in the brain with the higher affinity clone persisting longer in the host during chronic infection. Transcriptional profiling of naïve and activated ROP7-specific CD8 T cells revealed that *Klf2* encoding a transcription factor that is known to be a negative marker for T cell trafficking is upregulated in the activated lowest affinity ROP7 clone. Our data thus suggest that TCR–MHC affinity dictates memory CD8 T cell fate at the site of infection.

Keywords: CD8 T cells, *Toxoplasma gondii*, neurological infection and inflammation, T cell receptor–major histocompatibility complex interaction, ROP7

INTRODUCTION

CD8 T cells are a cornerstone of the adaptive immune defense to intracellular pathogens with their capacity to operate as antigen-experienced effector and memory cells. Pathogen-specific CD8 effector T cells rapidly expand and differentiate during the acute infection, followed by a phase of contraction and development of long-lived memory T cells (1, 2). Most of our understanding of T cell responses to chronic infections is derived from models where pathogen control is incomplete

and T cell become functionally impaired or exhausted over time (3, 4). We thus lack knowledge of what drives long-lasting control of chronically persistent pathogens.

The interaction of the T cell receptor (TCR) with the pathogen antigenic epitope loaded on the major histocompatibility complex (MHC) is essential in maintaining effective CD8 T cell control of persistent intracellular pathogens. The aβ TCR stochastically assembles and is selected during thymic development, and it is *via* this receptor that the immune system tunes the breath and strength of its response (2, 5). Efforts have been made to elicit the effect of TCR–MHC affinity on the fate of the resulting T cells, however, often this relied on varying the antigenic peptide rather the TCR (2, 6). The simple question of how T cells of different affinity to a given antigen fare during chronic infection remains unresolved.

To model a persistent chronic infection, we deemed a resistant mouse strain infected with the protozoan parasite *Toxoplasma gondii* to be most suitable. *Toxoplasma* is the most common parasitic infection in man, whereby in immunocompetent hosts the acute phase of infection is generally asymptomatic and proceeds to the chronic phase, which is incurable and defined by tissue cyst formation preferably in the brain. The parasite poses a serious health threat to immunocompromised individuals, especially AIDS patients. It is unclear how *Toxoplasma* maintains the intricate balance between survival and host defense. CD8 T cells and their ability to produce IFNγ have been shown to secure the latency of the parasitic infection (7, 8).

Mice harboring the MHCI allele H-2L^d (e.g., BALB/c) control *Toxoplasma* infection due to an immunodominant epitope derived from the GRA6 parasite protein (9–11). BALB/c mice exhibit very few tissue brain cysts and the functionality of their CD8 T cells in the *Toxoplasma*-infected brain is defined by their capacity to produce IFNγ and perforin (7, 12, 13). Recently, using the murine BALB/c chronic *Toxoplasma* model, a T cell population (T_{int}) in an intermediate state between effector and memory status was discovered, highlighting the value of this model for defining the fate of CD8 T cells during chronic infection with persistent antigen (14).

In addition to classical memory T-cell populations, a distinct memory T-cell population termed resident memory T cells (T_{RM}) has recently been documented. T_{RM} cells persist long term within non-lymphoid tissues, are resident in nature, self-renewing, and highly protective against subsequent infections (15, 16). These are and can be identified by CD103 expression (17, 18). Most T_{RM} cells to date have been characterized in mucosal tissue sites, where they are rapidly active against secondary infections (19–21). Much less is known about T_{RM} in the CNS. Viral models have defined CD8 T_{RM} in VSV encephalitis and in inoculation with LCMV (15, 20–22). In a susceptible C57BL/6 model of *Toxoplasma* infection, a transcriptionally defined resident memory CD8 population was recently defined in the brain (23). Again, prerequisites in terms of TCR–MHC affinity for the transition of CD8 T cells to a TRM phenotype are completely unexplored.

Rather than varying the antigenic peptide, we sought to use distinct clonal T cells. To answer how TCR–MHC affinity dictates trafficking and phenotype of memory CD8 T cells in the brain during chronic infection, we employed three distinct clonal CD8 T cells, each expressing a natural TCR recognizing the *Toxoplasma* antigen ROP7 (24, 25). These cells were obtained from transnuclear (TN) mice generated by somatic cell nuclear transfer from a nucleus of a *Toxoplasma* antigen-specific CD8 T cell and have different affinity for MHC class I loaded with the same ROP7 peptide (24, 25).

Here, we report that TCR–MHC affinity dictates the potential of a CD8 T cells to home to the *Toxoplasma*-infected brain. We employed three natural CD8 T cell clones derived from a resolving *Toxoplasma* infection by somatic cell nuclear transfer, defined to possess different affinities for the same *Toxoplasma* antigen ROP7 (24, 25). The two T cell clones with higher affinity, R7-I and R7-III, were found in the brain during chronic infection, while the lowest affinity clone R7-II was not, despite all three clones being activated during the acute phase of infection. As possible causes for this divergent homing, we observed high expression of the negative regulator of T cell activation *Klf2* and its regulated genes in peptide-activated R7-II T cells. In addition, *Ctla4*, a negative regulator of T cell responses, was also upregulated on R7-II T cells. The highest affinity clone, R7-I, persisted longer during the chronic phase of infection than R7-III and was able to generate more CD103$^+$ T cells in the brain. Thus, our results indicate that higher affinity of the TCR–MHC interaction is better for trafficking and persisting of the specific CD8 T cells at the site of chronic infection, here brain.

MATERIALS AND METHODS

Mice

Thy1.1 (BALB/c N4; CD90.1$^+$) and TN R7-I, -II, and -III mice on a Rag2 proficient BALB/c (Rag2$^{+/+}$CD90.2$^+$) background were housed and bred in the animal facility of the Francis Crick Institute (Mill Hill Laboratory, London, UK) (24). All procedures involving mice were approved by the local ethical committee of the Francis Crick Institute Ltd., Mill Hill Laboratory and are part of a project license approved by the Home Office, UK, under the Animals (Scientific Procedures) Act 1986.

Calcium Flux Assay

For calcium flux measurements, lymphocytes from lymph nodes (LN) of R7-I, -II, or -III mice were isolated and loaded with Indo-1 dye (Life Technologies) at concentration of 2 mg/ml in IMDM media containing 5% FCS for 40 min at 37°C. Subsequently, cells were washed two times with IMDM media and stained with anti-CD8 (53-6.7), anti-CD4 (GK1.5), and anti-CD3 (17A2) antibodies all from BioLegend (San Diego, CA, USA) for 20 min at room temperature. Lymphocytes were then stimulated by addition of ROP7–MHCI dextramer (Immudex) or by addition of Ionomycin (10 ng/ml).

ERK1/2 Phosphorylation Assay

For the ERK1/2 phosphorylation assay, lymphocytes from LN of R7-I, -II, or -III mice were isolated and stained with anti-CD8 (5H10, Invitrogen) and anti-CD4 (GK1.5, BioLegend) antibodies. Splenocytes loaded with ROP7 peptide were used as stimulators. Lymphocytes were then stimulated by addition of splenocytes

and incubated for 0, 1, 2, 4, 8, and 12 min at 37°C. At the indicated time points, cells were fixed with paraformaldehyde at a final concentration of 2%. Cells were permeabilized by addition of ice-cold 90% methanol and stored over night at −20°C. Next, cells were washed and stained with anti-pERK1/2 (pT202/pY204) (20A, BD Biosciences) and acquired using an LSR II flow cytometer. Data were analyzed using FlowJo and Prism software.

In Vitro Proliferation Assay

Splenocytes of R7-I, -II, and -III mice were isolated, stained with the intracellular fluorescent dye carboxyfluorescein diacetate succinimidyl ester (CFSE; 5 μM; Life Technologies) for 5 min at room temperature, and plated in 96-well plates. ROP7 peptide was added in the range of concentrations from 0.5×10^{-4} to 0.5×10^{-9} M. Three days later, cells were harvested and stained for FACS analysis.

T Cell Adoptive Transfer and Infections

Lymph nodes and spleens from TN ROP7 donor mice were harvested and the released cells negatively selected for CD8 T cells. Recipient Thy1.1 (BALB/c) mice received 10^6 ROP7$^+$ CD8 T cells *via* i.v. injection prior to infection. Mice were infected orally with five cysts of the ME49 *Toxoplasma* strain. Cells were harvested at the indicated time points during the acute and chronic phases of infection and processed accordingly.

Isolation of Brain Mononuclear Cells

Isolation of brain mononuclear cells was performed as described before (26). Briefly, mice were perfused with cold PBS, and brains were isolated and homogenized. Brain cell suspension was diluted to 30% with isotonic Percoll solution and layered on top of 70% isotonic Percoll solution. Gradients were spun for 30 min at 500 × *g*, 18°C. Mononuclear cell population was collected from the interphase of Percoll gradient, washed and resuspended for antibody staining or restimulation.

In Vivo Proliferation Assay

ROP7 CD8 T cells were prepared as described. Prior to subcutaneous injection into recipient mice, cells were stained with CFSE (5 μM). Mice were then infected orally as described. Spleen, LN, and mesenteric LN (mLN) tissues were then harvested 6/7 days post-infection (p.i.) and processed accordingly.

Ex Vivo Functional Assay

Cells harvested from mice 3 weeks p.i. were cultured *ex vivo* as a cell suspension for 2 h with Ionomycin (20 ng/ml) and PMA (1 μg/ml) after which Brefeldin A (2 μg/ml) was added for the next 2 h in RPMI media. Cells were then stained for flow cytometry and analyzed as described.

Micropipette Two-Dimensional Adhesion Frequency Assay

The two dimensional affinities were measured by micropipette adhesion frequency assay (27). CD8 T cells were negatively selected by magnetic cell sorting (Milteney) from spleen and LN of TN ROP7 mice. Human red blood cells (RBCs) were isolated in accordance with the Institutional Review Board at Emory University and used as the surrogate APC sensor through incorporation of ROP7 monomers with mouse β_2-microglobulin (National Institutes of Health Tetramer Core) *via* biotin:streptavidin interactions. RBCs were coated with Biotin-X-NHS (EMD, Millipore) and 0.5 mg/ml streptavidin (Thermo Fisher Scientific) and 1–2 mg of the monomer antigenic and control monomers. Monoclonal cells were brought into contact 50 times with pMHC coated RBCs with the same contact time and area (A_c), and the adhesion frequency (P_a) was calculated. Quantification of binding events along with TCR and pMHC surface densities and adhesion frequencies along with two-dimensional affinity were as described (27, 28).

Antibodies

Fluorescently labeled antibodies against CD3, CD90.1, CD90.2, CD62L, CD127, CD103, KLRG1, PD1 antigens, and IFNγ were purchased from BioLegend (San Diego, CA, USA). Fluorescently labeled antibodies against CD8 (5H10) alpha and anti-CD69 were purchased from Life Technologies (Carlsbad, CA, USA). H-2L^d monomers with IPANAGRFF or photo-cleavable peptide (YPNVNI(Apn)NF) were obtained from the NIH Tetramer Core Facility (Emory University, Atlanta, GA, USA) and were tetramerised and peptide-exchanged as described previously (29). All peptides were synthesized by Pepceuticals (Leicestershire, UK).

Flow Cytometry

Single-cell suspensions were prepared from brain, spleen, LN, and mLN by mechanical disruption. Brain mononuclear cells were isolated as described above (26). Cell were stained for 20 min at 4°C in an appropriate antibody cocktail and washed with PBS with 1% BSA. BD Cytofix/Cytoperm kit was used for intracellular staining of cells. Cells were run on a BD LSRII or BD Fortessa X20 and analyzed using FlowJo software (Tree Star).

Chimeras

Recipient BALB/c mice (CD90.1) were treated with an intraperitoneal injection of myeloablative agent Busulfan (10 mg/kg, Busilvex, Pierre Fabre) and injected with a congenic (CD90.2) donor bone marrow (BM) from ROP7 TN mice 1 day after to create BM chimeras. 6–8 weeks after BM transplantation chimerism was assessed in the blood to be up to 5% donor CD8 of total CD8 T cells. Donor CD8 T cells were 60–80% of total CD8 T cells in the thymus. Mice were infected orally with five cysts of *Toxoplasma* ME49.

RNASeq Analysis

Single-cell suspensions of splenocytes from R7-I, -II, or -III mice were incubated in RPMI medium 1640 supplemented with recombinant mouse IL-2 (10 ng/ml) overnight at 37°C with or without ROP7 peptide (10 μM). Cells were stained with live/dead, anti-CD3, anti-CD8a, and ROP7 tetramer. Live CD8$^+$ tetramer$^+$ T cells were sorted on the Aria, XDP, and Influx 1 cell sorters. Samples were maintained at 4°C and purity determined to be 90–95%. RNA was isolated using Trizol and the RNeasy Micro-Kit (Qiagen). A total of 200 ng of RNA was used to prepare the RNA library using TruSeq mRNA Library Prep Kit v2

(Illumina) according to the manufacturer's recommendations. RNA sequencing was performed on the Illumina HiSeq 2500 and typically generated ~25 million 100-bp non-strand-specific single-end reads per sample. The RSEM package (version 1.2.11) (30) was used for the alignment and subsequent gene-level counting of the sequenced reads relative to mm10 RefSeq genes downloaded from the UCSC Table Browser (31) on May 27, 2015. Differential expression analysis between the triplicate groups was performed with DESeq2 (version 1.8.1) (32) after removal of genes with a maximum transcript per million (TPM) value of 1 across all samples in the experiment. Significant expression differences were identified at a false discovery rate threshold of 0.01. Gene set enrichment analysis was performed by Gene Ontology Biological processes using GeneGo MetaCore (https://portal.genego.com/). All raw RNASeq sequence data and per sample TPM counts generated by RSEM can be accessed with GEO accession GSE88996 and GSE113827. Pathway analysis was performed using IPA software to demonstrate the biological effect of differentially expressed genes on cell cycle progression.

Real-Time PCR

RNA was extracted from ROP7-specific splenocytes, either straight from the spleen or incubated overnight with or without ROP7 peptide using RNeasy Mini and Micro Kits (Qiagen). cDNA was synthesized using the Maxima first strand cDNA synthesis kit for RT-qPCR, with dsDNase (Thermo Fisher Scientific).

Quantitative real-time PCR was performed using Maxima SYBR Green/Rox qPCR master mix (Thermo Fisher Scientific).

Results were normalized to the expression of CD8. Relative fold change was calculated by normalizing to the average of R7-I, R7-II or R7-III biological triplicates, respectively (straight from the spleen).

Primers used were as follows: KLF2 forward 5′-TGT GAGAAATGCCTTTGAGTTTACTG-3′, reverse 5′-CCCTTAT AGAAATACAATCGGTCATAGTC-3′, CXCR3 forward 5′-GC CAAGCCATGTACCTTGAG-3′, reverse 5′-GTCAGAG AAGTCGCTCTCG-3′, Sell forward 5′-ACGGGCCCCAG TGTCAGTATGTG-3′, reverse 5′-TGAGAAATGCCAGCCCC GAGAA-3′, S1P1 forward 5′-GTGTAGACCCAGAGTCCTG CG-3′, reverse 5′-AGCTTTTCCTTGGCTGGAGAG-3′, IL-6Rα forward5′-GTCACGGGCACTCCTTGGATAG-3′,reverse5′-AG GAATGTGGGCAGGGACATGG-3′, Itag4 forward 5′-GATG CTGTTGTTGTACTTCGGG-3′, reverse 5′-ACCACTGAGGC ATTAGAGAGC-3′, CXCR4 forward 5′-GACTGGCATAGTCG GCAATG-3′,reverse5′-AGAAGGGGAGTGTGATGACAAA-3′, IL-7Rα forward 5′-GCGGACGATCACTCCTTCTG-3′, reverse 5′-GCATTTCACTCGTAAAAGAGCCC-3′, CD8 forward 5′-GA TATAAATCTCCTGTCTGCCCATC-3′, reverse 5′-ATTCATAC CACTTGCTTCCTTGC-3′.

Statistical Analyses

GraphPad software (Prism) was used to perform statistical tests. Comparisons between two groups were made using Student's *t*-test. Comparisons between multiple groups were made using one-way analysis of variance test. Levels of significance are denoted as follows: $*p \leq 0.05$, $**p \leq 0.01$, $***p \leq 0.001$, and $****p \leq 0.0001$. Non-significant results are either not marked or indicated as NS.

RESULTS

Three CD8 T Cell Clones Specific for the Same Peptide Respond Differently to *In Vitro* TCR Stimulation With Cognate Antigen

We previously described TN mouse lines (24), which we used herein as a source of three CD8 T cell clones specific for the same peptide (IPAAAGRFF) derived from the ROP7 protein of *T. gondii*. We refer to these CD8 T cell clones as R7-I, R7-II, and R7-III CD8 T cells (24). We previously showed these CD8 T cell clones to differ in their TCR 3D affinity to cognate ROP7 peptide, with R7-I being the strongest binder at 4 μM and R7-II the weakest at 109 μM. R7-III has a binding affinity of 24 μM (25). To further define the kinetics of TCR signaling after stimulation with ROP7 peptide, we measured ER-driven calcium release, phosphorylation of ERK1/2 kinase, and cell proliferation as determinants of TCR reactivity. Both the calcium release and phosphorylation assays reflected the hierarchy of the TCR–MHC binding 3D affinity and were the fastest and strongest in R7-I CD8 T cells, while the R7-II CD8 T cell response was lowest (**Figures 1A,B**). In addition, we noted that R7-II CD8 T cells had a basal level of free intracellular calcium that was higher than that of R7-I and R7-III CD8 T cells (**Figure 1A**). As a positive control, we used CD3 cross-linking to stimulate R7 cells (Figure S1 in Supplementary Material). All three clones are able to phosphorylate ERK1/2 kinase equally upon CD3 cross-linking (Figure S1A in Supplementary Material). Calcium release upon CD3 cross-linking was lower for R7-II and equal for R7-I and R7-III (Figure S1B in Supplementary Material). In the *in vitro* proliferation assay, R7-II CD8 T cells were not able to proliferate efficiently even at the highest (500 μM) concentration of ROP7 peptide loaded onto splenocytes, while R7-I and R7-III CD8 T cells reached the highest division index at concentrations 5 and 0.5 μM, respectively (**Figure 1C**). We previously conducted *ex vivo* proliferation experiments of R7 CD8 T cells crosslinked on plate-bound CD3/CD28 and concluded that R7-II cells barely proliferated at all (25). Combined, these *in vitro* experiments suggest that the 3D surface plasmon resonance affinity of the TCR–MHC binding reflects the strength of downstream signaling and partially translates to proliferation capacity *in vitro*.

To provide additional insight into the functional response of the three R7 CD8 T cell clones during *Toxoplasma* infection, we determined their 2D affinity for the ROP7 antigen. The micropipette adhesion frequency assay provides 2D-based measures of TCR affinity for pMHC in a context that is membrane anchored. 2D affinity correlates more closely to functional responses than do 3D affinity measurements whose measurements are based on purified proteins. Over 40 T cells for each clone were analyzed to reveal similar high affinities for R7-I and R7-III (geometric means being 1.38E−04 and 1.27E−04, respectively) and that R7-I whilst having a similar affinity to R7-III (**Figure 1D**) has a higher adhesion frequency than R7-III (**Figure 1E**) that being 0.91 and 0.81, respectively. R7-II had a threefold lower 2D affinity (7.01E−05). The threefold difference in affinity is functionally relevant as previously, we have demonstrated that during Polyoma infection CD8 T cells with the highest 2D affinity are found in the CNS

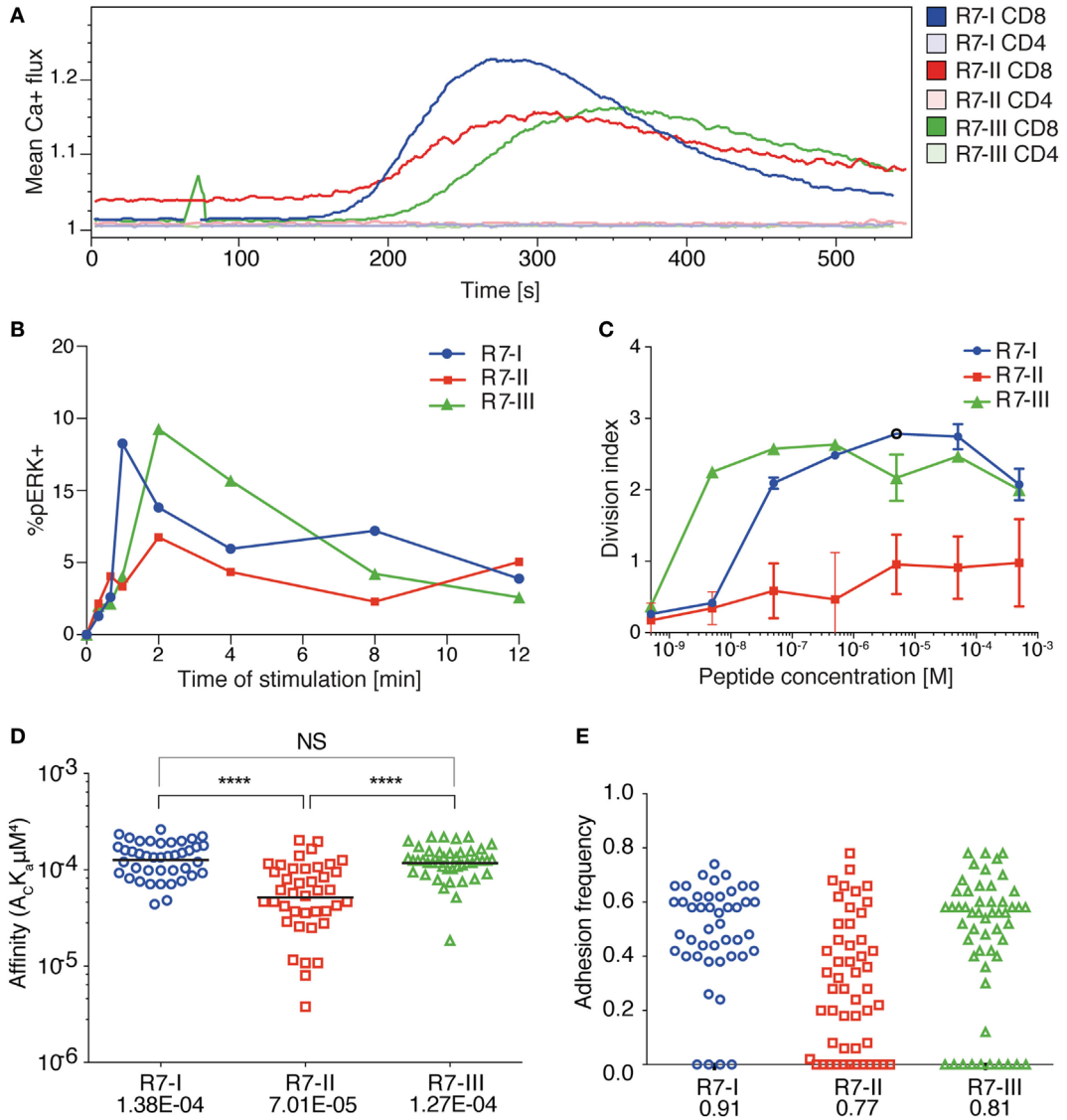

FIGURE 1 | Three distinct CD8 T cell clones of the same specificity exhibit different 2D affinity and responses to specific TCR receptor stimulation. **(A)** Ca^{2+} flux profile of the three R7 CD8 T cell lines upon stimulation of TCR signaling with ROP7 dextramer (representative of two experiments with multiple mice each). **(B)** Phosphorylation of ERK1/2 kinase in time upon stimulation with splenocytes loaded with ROP7 peptide (representative of two experiments). **(C)** Proliferation of R7 CD8 T cells after stimulation with a range of ROP7 peptide concentrations (representative of three experiments). **(D)** Relative 2D affinity of the three R7 CD8 T cell clones specific for ROP7 (IPAAAGRFF) normalized by TCR surface density. Each individual data point represents the affinity for a single CD8 T cell. Analysis utilizes the geometric mean of the population. **(E)** Adhesion frequencies of the three ROP7 clones F. Gaussian curves were fitted to the affinities of **(D)**. Blue line represents R7-I, red line represents R7-II, and the green line represents R7-III. Data are cumulative from two individual experiments and a total of three mice per clone.

and eventually comprise the T_{RM} population (33). In addition, we have reported CD4 T cells mediating EAE carry a twofold higher affinity when compared with the peripheral T cells (34).

All Three Clones of R7 CD8 T Cells Are Efficiently Primed in the Acute Phase of *T. gondii* Infection

Next, we sought to verify if these differences observed *in vitro* would still hold true *in vivo*. R7 CD8 T cells were adoptively transferred into congenic naïve recipient mice (CD90.1 BALB/c). Subsequently, mice were orally infected with ME49 *Toxoplasma* tissue cysts. The donor R7 CD8 T cells could then be followed during the acute and chronic phase of infection (**Figure 2A**). We were able to observe proliferated cells for all three R7 clones in the mLN earliest 6 days p.i. (**Figure 2B**). The numbers of R7-II donor cells found in the mLN and spleen were at least 10 times lower than numbers of other two clones (**Figure 2B**). However, those R7-II cells that were recovered from mLN had low CFSE level indicating that they had proliferated similarly to R7-I and R7-III CD8 T cells. In addition, the R7 donor CD8 T cells were all activated to the same extent based on CD69 expression

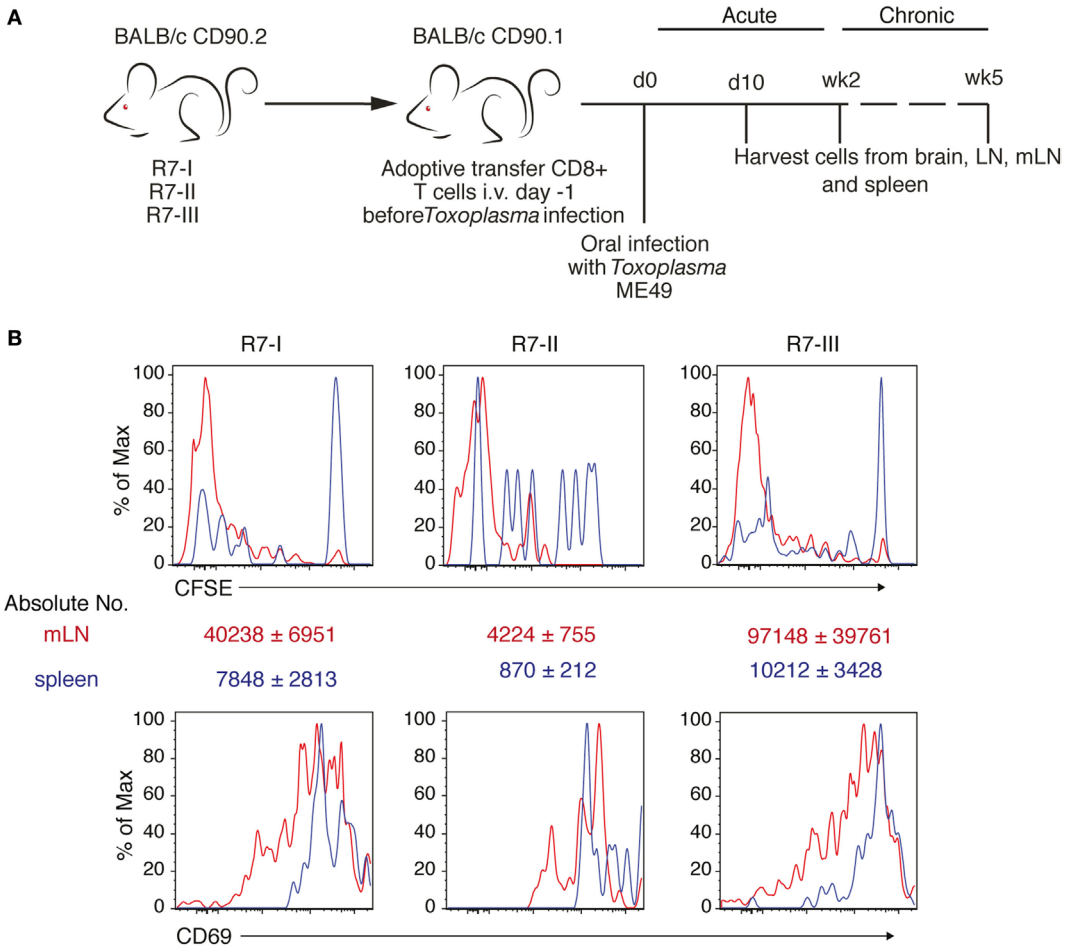

FIGURE 2 | Three clones of R7-reactive CD8 T cells are primed and activated during the acute phase of *Toxoplasma gondii* infection. **(A)** Schematic diagram of the experimental setup for *in vivo* experiments. Transnuclear R7 mice were used as a donor of CD8 T cells in adoptive transfer experiments (AT). CD8 T cells isolated from lymph nodes (LN) and spleens were transferred to congenic recipients. Recipient mice were infected orally with five cysts of *Toxoplasma* ME49. At different time points post-infection (p.i.) recipient mice were sacrificed and donor CD8 T cell populations were assessed. **(B)** Donor cells were stained with CFSE before transfer. Histograms show CFSE dilution and CD69 expression on transferred R7 CD8 T cells isolated from mesenteric LN (mLN) 6 days p.i. *via* the oral route (representative of two independent experiments).

(**Figure 2B**). We conclude that all three R7 clones are responsive to a *Toxoplasma* infection *in vivo*, as measured by proliferation and activation status.

R7-II CD8 T Cells Do Not Persist and Do Not Reach the Brain of Recipient Mice During *T. gondii* Infection

Cysts in the brain characterize the chronic phase of *Toxoplasma* infection. IFNγ produced by CD8 T cells is crucial for the maintenance of the quiescent cyst form of *Toxoplasma* (8, 13). We showed that the three R7 CD8 T cell clones could be primed and proliferated in the acute phase of *Toxoplasma* infection. Next, we investigated if R7 CD8 T cells could be found in the brain in the chronic phase of *Toxoplasma* infection. We analyzed brain, spleen, mLN, and non-draining LN for the presence of transferred R7 CD8 T cells 3 weeks p.i. R7-I and R7-III CD8 T cells were found in significant numbers in the brain at 3 weeks p.i. (**Figure 3A**). Percentages and absolute numbers of donor R7 CD8 T cells of all CD8 T cells in a given organ were different depending on the clone (**Figure 3A**). The R7-II clone was found in insignificant percentages and numbers in all tested organs. R7-I and R7-III clones were present in higher percentages from 2 to 15% of all CD8 T cells depending on the organ. There was no significant difference between percentages of the R7-I and R7-III clone in the brain. In the spleen and mLN, we observed significantly higher percentages of the R7-III CD8 T cells. We also determined absolute cell number for each clone at each site and did not observe significant differences between the R7-I and R7-III clone (**Figure 3A**, right panel).

We analyzed earlier time points to estimate the time when donor cells reached the brain and to assess if there is a difference in donor cell number or percentages in the acute phase of infection. R7-I and R7-III CD8 T cells were observed in the brain as early as

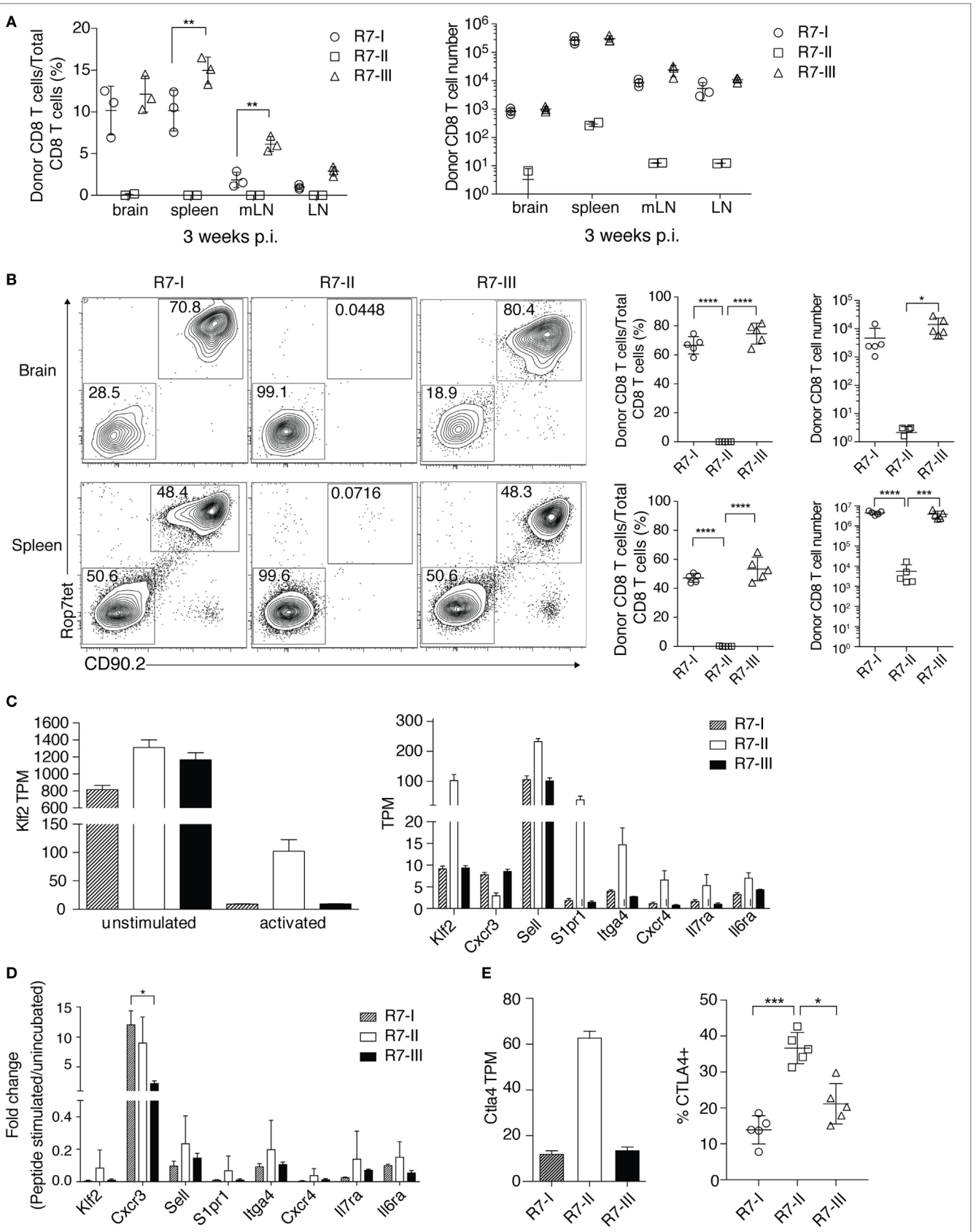

FIGURE 3 | Continued

FIGURE 3 | R7-II CD8 T cells do not persist and do not reach the brain of recipient mice during *Toxoplasma gondii* infection. **(A)** Percentages and total cell numbers of donor R7 CD8 T cells in the brain and lymphoid organs 3 weeks post-infection (p.i.) (representative of at least five experiments with three mice per line), only significant relationships between R7-I and R7-III CD8 T cells are shown, $*p \leq 0.05$, $**p \leq 0.01$, $***p \leq 0.001$, two-way analysis of variance (ANOVA) followed by multiple comparisons Tukey's. Mean and SD. **(B)** Percentages and cell numbers of donor R7 CD8 T cells in the brain and spleen in the acute phase of infection (day 10 p.i.) (representative of two experiments), $*p \leq 0.05$, $**p \leq 0.01$, $***p \leq 0.001$, one-way ANOVA followed by multiple comparisons Tukey's. Mean and SD. **(C)** Splenocytes of R7 mice were left untreated (unstimulated) or stimulated with the Rop7 peptide (activated) over night. On the next day, ROP7tet$^+$ CD8 T cells were sorted and lysed for RNA extraction. Transcripts levels were evaluated in an RNAseq experiment. Klf2 was upregulated in activated R7-II by a fold change of 8.8 over activated R7-III (**Table 1**). Expression of *Klf2* and Klf2-regulated genes is shown as transcript per million (TPM) in unstimulated and activated (left hand graph) or only activated R7 CD8 T cells (right graph). **(D)** Validation of RNAseq results was performed on samples from an independent experiment with use of qRT-PCR. Expression of *Klf2* and Klf2-regulated genes shown as normalized $2^{-\Delta\Delta Ct}$ values. $*p \leq 0.05$, one-way ANOVA followed by multiple comparisons Tukey's. Mean and SD. **(E)** *CTLA4* expression in the RNAseq experiment shown as TPM value in activated samples (left graph) and CTLA4 protein expression evaluated by FACS of cells isolated 5 days p.i. from lymph nodes (LN) of mice adoptively transferred with R7 cells and infected with *Toxoplasma* (right graph). $*p \leq 0.05$, $**p \leq 0.01$, $***p \leq 0.001$, one-way ANOVA followed by multiple comparisons Tukey's. Mean and SD.

10 days p.i., however, we failed to detect a distinct R7-II CD8 T cell population in the brain (**Figure 3B**). R7-II CD8 T cells could not be observed in prominent numbers in any of the tested primary and secondary lymphoid organs suggesting a lack of proper expansion and thus an absence of the transferred population in the brain (**Figure 3B**; Figure S2A in Supplementary Material). Combining our previous observations of the low TCR–MHC affinity of R7-II cells (**Figures 1D,E**) and the low proliferation in response to *in vivo* stimulation during a *Toxoplasma* infection (**Figure 2B**), we concluded that R7-II cells most likely fail to expand sufficiently in secondary lymphoid organs to efficiently home to the brain. R7-I and R7-III CD8 T cells were a major part (60–80%) of the total CD8 T cell population in the brain at day 10 p.i. Their percentages decreased throughout time during which host CD8 T cells reached the brain suggesting that the transferred T cell clones exhibited a rapid recruitment to the brain compared to newly formed *Toxoplasma*-specific CD8 T cells of the host. There were no significant differences in percentages or numbers of donor population between R7-I and R7-III CD8 T cells at day 10 or 2 weeks p.i. (**Figure 3B**; Figure S2A in Supplementary Material).

To dissect the reasons for the poor expansion and lack of R7-II cells in the brain we compared the transcriptional profiles of *in vitro* ROP7-activated R7-II vs R7-I or R7-III cells. As expected, the global gene expression differences were much more pronounced when peptide-activated R7-II cells were compared with R7-I and R7-III (Figure S3 in Supplementary Material). In the list of the top 10 genes upregulated in R7-II (**Table 1**), we found *Klf2* encoding a transcription factor that is known to be important for T cell trafficking between the blood and lymphoid organs (35–37). Klf2 is highly expressed in naïve and memory T cells but downregulated in effector T cells upon binding of the TCR to its cognate peptide (38). The stronger the binding affinity, the lower the expression of *Klf2* and the better the activation of the T cells (39). In addition, *S1pr1* which is regulated by Klf2 was also in the top 10 upregulated genes. We analyzed the expression of *Klf2* across the unstimulated and activated samples of the RNASeq experiment (**Figure 3C**, left graph) as well as at the genes known to be regulated by Klf2 such as *CXCR3, Sell (CD62L), S1pr1, Itga4, CXCR4, Il7ra*, and *Il6ra* (**Figure 3C**, right graph). *Klf2* expression was at similar level in all three naïve CD8 T cell clones. After activation, all three clones downregulated *Klf2*, however, downregulation in R7-II was the weakest reflecting the lowest binding affinity of Rop7 peptide to R7-II. Expression of *Sell (CD62L), S1pr1, Itga4, CXCR4, Il7ra*, and *Il6ra* mirrored *Klf2* expression being highest in R7-II and was comparable between R7-I and R7-III. On the other hand, *CXCR3* expression was lowest in R7-II. We performed an independent *in vitro* activation experiment and observed a similar trend of gene expression by qRT-PCR as seen in the RNAseq results (**Figure 3D**). mRNA expression detected by qRT-PCR correlated with the RNAseq data for all tested genes except the *CXCR3* gene.

CTLA4 is known as a negative regulator of T cell responses. We analyzed the expression of the *Ctla4* transcript in the RNASeq of activated ROP7 CD8 T cells as its high expression in R7-II cells could explain their poor performance in proliferation capacity and subsequent lack of homing to the brain. As expected,

TABLE 1 | Top 10 up and downregulated genes in activated R7-II vs R7-I and R7-III.

	Gene symbol	FC	FDR
Up in R7-II (FC > 2,531 genes)			
1	Tnfrsf19/CD137	19.20	5.84E−105
2	Mturn	14.93	1.95E−77
3	Rasgrp2	13.49	1.27E−90
4	Slc6a19	12.84	2.18E−44
5	Cd7	11.38	4.03E−49
6	S1pr1	9.77	1.21E−44
7	Nsg2	9.68	3.28E−34
8	Klf2	8.80	4.88E−149
9	Atp6v0e2	8.60	1.18E−29
10	Arl4c	8.45	5.70E−105
Down in R7-II (FC > 2,119 genes)			
1	Tbx21/Tbet	−6.45	4.64E−38
2	Tnfsf11/RANKL	−6.07	5.80E−160
3	Serpinb6b	−5.64	2.11E−42
4	Dapl1	−5.51	1.15E−38
5	Ccl9	−5.46	3.81E−93
6	Rnf157	−4.89	5.80E−78
7	Tbkbp1	−4.51	2.74E−32
8	Lipg	−4.51	4.47E−72
9	Stc2	−4.14	8.38E−16
10	Chst11	−3.95	1.98E−56

Table shows top 10 up- and downregulated genes in R7-II samples as compared with R7-I and R7-III samples upon activation, where only genes differentially expressed in R7-II vs R7-I and R7-II vs R7-III comparisons but similar expression between R7-I and R7-III were included. For each gene in the table, fold change (FC) and false discovery rate (FDR) are shown for R7-II vs R7-III comparison.

we observed the highest expression of *Ctla4* in R7-II CD8 T cells in comparison with the two other R7 clones (**Figure 3E**, left graph). We could confirm the RNAseq data in an *in vivo* experiment, where R7 T cells were adoptively transferred to congenic mice and analyzed in LNs 5 days after infection with *Toxoplasma*. CTLA4 surface expression determined by FACS in R7-II cells was highest in comparison to R7-I and R7-III CD8 T cell clones (**Figure 3E**).

R7-III Has a Higher Contraction Rate and Does Not Persist in the Late Phase of Chronic Infection

At 5 weeks p.i. compared with 3 weeks p.i., we observed a dramatic decrease in the R7-III CD8 T cell population in all of tested lymphoid and non-lymphoid organs while the R7-I CD8 T cell population decreased more subtly, which could be explained by natural contraction of the population after an initial expansion phase (**Figure 4A**; Figure S2B in Supplementary Material).

The formation of memory CD8 T cells in persistent infections is still controversial (40). In BALB/c mice where persistent *Toxoplasma* infection is known to be controlled by CD8 T cells (13), the presence of memory CD8 T cells is expected. We analyzed if R7 CD8 T cells differentiated into memory cells and if the ratio of differentiation into effector and memory precursors was the same between R7-I and R7-III CD8 T cells. Short-lived effector cells (SLEC, $CD127^{-}KLRG1^{+}$) were present in similar percentages in R7-I and R7-III CD8 T cell populations in the brain and spleen at 3 and 4 weeks p.i. (**Figure 4B**). Memory precursor effector cells (MPEC, $CD127^{+}KLRG1^{-}$) where not present at 3 weeks p.i., however, we detected population of MPEC at 4 weeks p.i. in the spleen in similar percentages between R7-I and R7-III CD8 T cell (**Figure 4B**, bottom panel).

In the chronic phase of *Toxoplasma* infection in C57BL/6 mice, CD8 T cells in the brain are exhausted and express high levels of the exhaustion marker PD1 (41). Blockade of the PD1–PDL1 pathway has been shown to rescue the exhaustion phenotype of CD8 T cells and prevent mortality of chronically *Toxoplasma*-infected animals (42). In contrast to C57BL/6 mice, BALB/c mice are resistant to chronic *Toxoplasma* infection (9) and *Toxoplasma* GRA6-specific CD8 T cells in BALB/c mice lack PD1 expression during the chronic phase (14). We investigated if R7 CD8 T cells in brain of BALB/c mice at 3 weeks p.i. were exhausted. Almost 90% of R7 CD8 T cells expressed PD1 (**Figure 4C**). No significant difference was observed between R7-I and R7-III CD8 T cell populations in the brain suggesting that it is not exhaustion that leads to greater contraction of the R7-III CD8 T cell population. As PD1 can be also a marker for recently activated cells, we analyzed the ability of $PD1^{+}$ cells to produce IFNγ, since cytokine production is lost in a truly exhausted cell (43). Brain mononuclear cells from week 3 of infection were *ex vivo* re-stimulated with PMA and ionomycin and stained for IFNγ (**Figure 4C**). More than half of PD1 positive cells were able to produce IFNγ and only 1/3 of R7 CD8 T cells in the brain were positive for PD1 and negative for IFNγ. At the same time, only 5% of R7 cells in spleen expressed PD1 and did not produce IFNγ. No significant difference between R7-I and R7-III CD8 T cells was observed indicating that the reason for the disappearance of R7-III CD8 T cells is independent of their exhaustion state.

Next, we considered CXCR3 as a candidate molecule to unravel the differences in persistence between R7-I and R7-III. The CXCR3 receptor is important in trafficking of CD8 T cells to non-lymphoid tissues including the brain (44). We evaluated CXCR3 expression levels on R7-I and R7-III CD8 T cells during *Toxoplasma* infection. CXCR3 expression on R7-III CD8 T cells was significantly lower at day 10 p.i. both in the brain and in the spleen (**Figure 4D**). However, no difference in CXCR3 expression was observed at 3 weeks p.i., thus it is questionable if lower CXCR3 expression at earlier time points of infection were the driver for lower R7-III CD8 T cell numbers observed in the brain at 5 weeks p.i.

To better understand the observed decrease in the brain population of R7-III CD8 T cells we set up BM chimeras. We used the transplant conditioning drug busulfan to induce myeloablation and create a niche for the R7-I or R7-III BM (45). In the brain and spleen, R7-I and R7-III BM chimeras have similar percentages of CD8 T cells originating from the donor's BM at both week 3 and 5 p.i. (**Figure 4E**). These results show that constant replenishment from the periphery is necessary for the persistence of donor cells is the brain at 5 weeks p.i. When R7-III CD8 T cells disappear from the periphery, they also disappear from the brain. By creating chimeras, we showed that when we keep a constant R7-III population in the periphery these cells also persist in the brain.

R7-I CD8 T Cells of T_{RM}-Like ($CD103^{+}$) Phenotype Are Present in Higher Percentages in the Brain Than R7-III CD8 T Cells

Previous studies have shown that tissue-resident memory T cells found in the brain long after acute infection has been cleared can survive without replenishment from the CD8 T cells circulating in the blood (15). We analyzed $CD69^{+}$ $CD103^{+}$ T cells in our model of chronic *Toxoplasma* infection. We observed a higher percentage of donor $CD103^{+}$ cells compared with total donor CD8 T cells for R7-I compared with R7-III at 3 weeks p.i. in the brain (**Figure 5A**). There was no significant difference between the total numbers of R7-I and R7-III $CD103^{+}$ cells in the brain. At week 5 p.i., about 80% of R7-I cells compared to the total donor CD8 T cell population had a T_{RM}-like phenotype (**Figure 5B**). The total number of donor R7-I cells stays stable between week 3 and 5 p.i. (**Figure 4A**, right), while we observed an increase in percentages and numbers of R7-I $CD103^{+}$ cells. As expected, R7-III $CD103^{+}$ cells at 5 weeks p.i. were not found in the brain.

We show with our BM chimera experiment that R7-III cells in the brain are replenished from the periphery (**Figure 4E**). BM chimeras 3 weeks p.i. also exhibited lower percentages of R7-III $CD103^{+}$ cells in the brain (**Figure 5C**), suggesting that the difference to produce less T_{RM}-like cells is intrinsic to the R7-III.

DISCUSSION

Affinity of TCR–MHC interaction influences the fate of the activated T cell (2). Immediate effects of strong or weak interactions

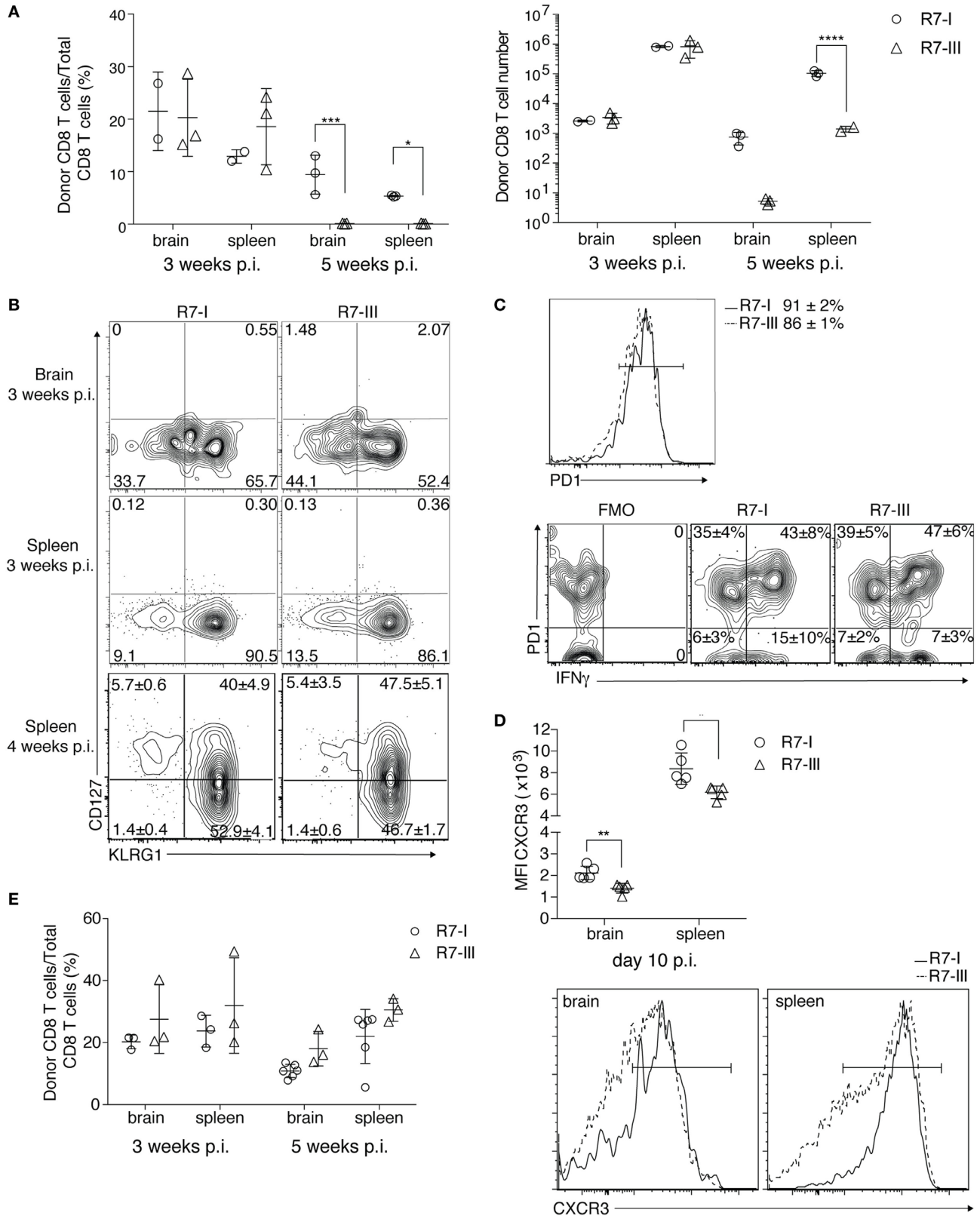

FIGURE 4 | Continued

FIGURE 4 | R7-III has a higher contraction rate and does not persist into the late phase of chronic *Toxoplasma gondii* infection. ROP7 CD8 T cells were adoptively transferred into congenic mice before *Toxoplasma* infection. Spleen, mesenteric LN and popliteal and axillary lymph nodes and brains were harvested and analyzed by flow cytometry **(A–E)**. **(A)** Percentages and total cell numbers of donor Rop7 CD8 T cells in the brain and spleen 3 and 5 weeks post-infection (p.i.) (representative of at least five experiments with two or three mice per cell line per experiment). $*p \leq 0.05$, $**p \leq 0.01$, $***p \leq 0.001$, two-way analysis of variance followed by Tukey's multiple comparisons test. **(B)** Donor population was assessed for expression of CD127 (IL7Ra) and KLRG1 at 3 and 4 weeks p.i. (representative of at least five experiments). **(C)** PD1 expression on donor CD8 T cells in the brain 3 weeks p.i. and their potential to produce IFNγ after *ex vivo* restimulation with PMA/Ionomycin (representative of two experiments). $*p \leq 0.05$, $**p \leq 0.01$, $***p \leq 0.001$ by Student's *t*-test. **(D)** CXCR3 surface staining on donor CD8 T cells 10 days p.i. in brain and spleen together with representative histogram plots of CXCR3 expression of donor R7 CD8 T cells in the brain and spleen 10 days p.i. **(E)** Percentages of R7 CD8 T cells in brain and spleen of R7 bone marrow chimeras at 3 and 5 weeks (minimum of three mice analyzed per condition) p.i. $*p \leq 0.05$, $**p \leq 0.01$, $***p \leq 0.001$ by Student's *t*-test.

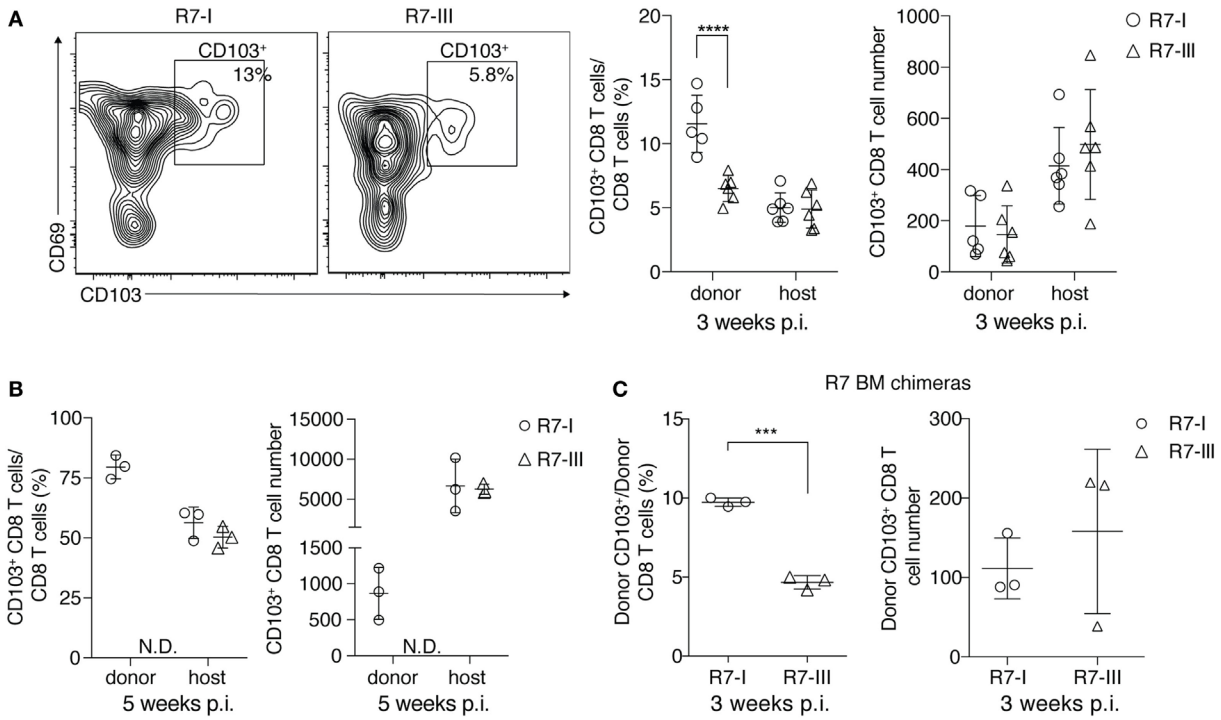

FIGURE 5 | R7-I CD8 T cells of a T_{RM}-like phenotype (CD103+) are present in higher percentages in the brain of *Toxoplasma gondii*-infected mice than R7-III CD8 T cells. ROP7 CD8 T cells were adoptively transferred into congenic mice before *Toxoplasma* infection **(A,B)**. **(A)** Representative FACS plots of donor CD103+ memory population in the brain at 3 weeks post-infection (p.i.) are shown on the left. Percentages and numbers of donor and host CD103+ CD8 T cells in the brain 3 weeks p.i. are shown on the right (graphs shows pooled results from two experiments and are representative of at least five experiments with two or three mice each). $***p < 0.001$ by Student's *t*-test. **(B)** Percentages and numbers of donor and host CD103+ CD8 T cells in the brain 5 weeks p.i. are shown (graphs are representative of at least three experiments with two or three mice each). N.D. denotes populations not detected. $*p \leq 0.05$, $**p \leq 0.01$ by Student's *t*-test. **(C)** CD103+ percentages and numbers in brains of R7 bone marrow chimeras mice 3 weeks p.i., three mice per T cell line, $*p \leq 0.05$, $**p \leq 0.01$, $***p \leq 0.001$ by Student's *t*-test.

on activation and expansion of the T cells have been studied broadly (2, 46, 47). However, it is unclear how affinity influences memory CD8 T cell formation. Herein, we studied three different clones of CD8 T cells (R7-I, -II, and -III) during *Toxoplasma* infection in BALB/c mice. These three CD8 T cell clones harbor TCRs specific for the same peptide of the *Toxoplasma* protein ROP7, but differ in their sequence and affinity for that peptide presented in MHC class I (24, 25). The hierarchy of affinity and functional *in vitro* responsiveness to ROP7–MHCI of the clones was R7-I > R7-III > R7-II (25). The lowest affinity clone R7-II failed to traffic to the brain during the chronic phase of infection even though we could show acute phase proliferation. R7-I outperformed R7-III in persistence in lymphoid organs and the brain in chronic infection. In addition, R7-I was able to form more resident memory T cells in the brain than R7-III.

To test the affinity of the three R7 CD8 T cell clones in a more physiological setting, in addition to our previously published 3D affinity measurements, we performed 2D affinity measurements. Interestingly, we demonstrated little affinity difference between R7-I and R7-III. However, R7-I had a higher adhesion frequency than R7-III, possibly explaining the functional differences we observed between these clones in the chronic phase of infection.

R7-II, the clone with the lowest affinity for ROP7 peptide, was not found in the chronic state of *Toxoplasma* infection. Small

number of the cells of that clone got activated and proliferated in the acute phase of infection, but after the contraction phase that clone could not be found neither in any analyzed lymphoid organs nor in the brain. As one possible hypothesis, we demonstrated by RNAseq and subsequent qPCR that R7-II did not cross the affinity threshold required to downregulate *Klf2* levels and consequently set the cells for homing to infected tissues. Lack of homing and retention in the LN as a mechanism responsible for lack of R7-II in brain was also supported by increased CTLA-4 expression. CTLA-4 expression on T cells is known to be responsible for cells being retained the LN after antigen encounter and mark anergic cells (48, 49). It is considered as one of T cell-intrinsic function of CTLA-4 to control self-reactive T cell motility in tissues (50). Signals from week TCR–MHC interaction may prevent full activation of the T cell, but still enable it to receive partial signals (2). Little is known about transcriptional regulation of *Ctla-4* (51). It has not been investigated if Klf2 can directly or indirectly regulate Ctla-4 expression.

R7-I and R7-III clones were of higher affinity than the R7-II clone and both were found in the brain during the chronic phase of infection. The initially quite similar clones performed differently in the later phase of infection. While both clones were able to form SLEC and MPEC cells, the R7-III clone did not persist in the periphery and brain in the later phase of chronic infection. In addition, in the brain, more R7-I than R7-III cells showed a phenotype of resident-like memory cells ($CD69^+CD103^+$). We postulate that these differences can be attributed to the increased adhesion frequency we observed in 2D measurements, as well as the increased TCR–MHC binding affinity exhibited in 3D measurements (25). We were not able to exactly pinpoint the reason for the disappearance of R7-III cells during the chronic phase of infection. It could be attributed to slower replication, higher rate of death, or formation of different types of cells that have different abilities to survive.

R7-III has been shown to be more proliferative than R7-I (more cell cycle terms in GO analysis) (25). Also, we observed slightly higher percentages of R7-III than R7-I cells in the spleen at 3 weeks p.i. indicating that the initial slower replication rate of R7-III is not the reason for differences between R7-I and R7-III observed in the later chronic phase of infection. SLEC and MPEC percentages were not significantly different between two clones. In addition, the expression of the exhaustion marker PD-1 and the ability to produce IFNγ also did not differ between R7-III and R7-I at 3 weeks p.i.

Creating BM chimeras, we provided an artificial model where R7-specific CD8 T cells are routed from the BM *via* the thymus to the periphery also during infection. This phenomenon has been described in persistent viral infections where host cells, but not donor cells, can be resupplied through thymic output, and new, naive specific CD8 T cells are being generated and subsequently primed during persistent infection (52). Newly generated T cells preserve antiviral CD8 T cell populations during chronic infection (52). In the C67BL/6 mice model of *Toxoplasma* infection T cells are recruited from the periphery to the brain in the chronic stage (41).

In our BM chimeras model, even if cells get exhausted or/and stop dividing, new R7-specific cells are available to traffic to the brain. We concluded that constant replenishment from the periphery is necessary to keep the population of R7-III in the brain in the later stages of chronic infection. If the cells are available in the periphery they will traffic to the brain. Thus, since the R7-I clone exhibits longer survival in the periphery and in the brain, we can conclude that cells of stronger affinity perform better in chronic infections.

The proportion of the cells with T_{RM}-like phenotype was different between R7-I and R7-III donor population in the brain. R7-III cells persistently exhibited a lower percentage of T_{RM}-like cells, no matter if able to replenish from the periphery in BM chimeras or not. In addition, R7-III cells exhibiting the phenotype of resident-like memory T cells ($CD69^+CD103^+$) at 3 weeks p.i. were absent from the brain at 5 weeks p.i. This suggests that these were possibly not true (classical) T_{RM} cells that are long lasting and shown to persist for years after infection. However, "classical" T_{RM} were defined in acute infection models with rechallenge or persisting but latent virus infection (HSV) (20, 53–56). Beura et al. show that T_{RM} from chronic infections differ from these analyzed in the acute infections with not only distribution in different non-lymphoid tissues but also expression of CD69 and CD103 markers (57). It is thus conceivable that in chronic infection they may have a different characteristic. Constant antigen stimulation during persistent infection may have a negative influence on T_{RM} that are considered to be antigen independent. Persistent antigen stimulation has been shown to lower CD103 expression on T_{RM} but it did not block their formation (55). It is possible that these cells become exhausted when constantly stimulated and thus only newly formed CD103-positive cells contribute to the cells observed in the brain (23). The strength of the antigen stimulation can influence this process and lower affinity could lead to lower number of R7-III cells expressing CD103, eventually leading to the elimination of these cells. Indeed, it has been shown that T_{RM} in the brain exhibit about 20-fold higher affinity as compared to splenic memory cells (33). As in our model R7-I and R7-III CD8 T cell differ in their TCR receptor, we propose that observed differences to persist as T_{RM}-like cells are mostly due to cognate peptide affinity. One caveat is, however, that this difference may not only be derived from the affinity of the interaction with the cognate ROP7 peptide, but different TCRs may already shape the fitness of the cells differently in the thymus (25, 58). Indeed, we previously showed that R7-I and R7-III cell respond differently to CD3/CD28 stimulation with R7-III is being more proliferative. Thus, the self-reactivity of T cells may also play a role in the later stages of an infection in shaping the memory CD8 T cell phenotype.

Effector T cells in chronic infection are constantly exposed to antigen leading to exhaustion (59, 60). In the *Toxoplasma* infection model of C57BL/6 mice, it has been shown that chronic infection leads to exhaustion of CD8 T cells in the brain (42, 61). However, C57BL/6 mice, unlike BALB/c mice are not resistant to *Toxoplasma* and die in the chronic phase of infection (42, 61). BALB/c mice, which we used in our model, are resistant to *Toxoplasma* and the chronic stage of infection is asymptomatic in this mouse strain. This implies that CD8 T cells in the BALB/c model are not exhausted. Indeed, recently published data by Chu et al. show that CD8 T cells specific for

the immunodominant GRA6 epitope are not exhausted (14). The ROP7 epitope is subdominant, but has been shown to be well-represented in the chronic phase of infection (29). We observed high levels of PD-1 expression on brain R7-specific CD8 T cells. However, the majority of these cells was able to produce IFNγ and could not be perceived as exhausted. The expression of PD-1 in this case may indicate recent antigen encounter, which is not surprising in chronic infection. In contrast with what was shown for Gra6-specific cells (14), our results indicate that CD8 T cells specific for subdominant epitopes do go through a contraction phase during chronic infection. R7-I and R7-III contraction happens after a peak in T cell numbers on days 14–21.

We conclude that R7-III cells, due to their lower affinity for the ROP7 peptide form less T_{RM}-like cells and do not persist in the later stages of chronic infection. Our data indicate that among cells specific for the subdominant antigen the cells of higher affinity are favored and their persistence is secured by formation of long-lasting T_{RM}-like cells in the non-lymphoid tissues.

ETHICS STATEMENT

All procedures involving mice were approved by the local ethical committee of the Francis Crick Institute Ltd., Mill Hill Laboratory and are part of a project license approved by the Home Office, UK, under the Animals (Scientific Procedures) Act 1986.

AUTHOR CONTRIBUTIONS

AS, NY, and E-MK conducted experiments. AS, NY, E-MK, HP, and BE analyzed the data. BE provided essential technology. AS and E-MF wrote the manuscript. E-MF directed the study.

ACKNOWLEDGMENTS

We acknowledge the NIH Tetramer Core Facility (contract HHSN272201300006C) for provision of H2Ld monomers with IPANAGRFF and photo-cleavable peptides. We would like to thank Blake Gibson for technical assistance. We are indebted to the Mill Hill Biological Services and FACS facility. We would like to thank Ben Seddon, George Kassiotis, Jean Langhorne, Charles Sinclair, Thea Hogan, and Jie Yang for discussion. This work was supported by the Francis Crick Institute, which receives its core funding from Cancer Research UK (FC001076), the UK Medical Research Council (FC001076), and the Wellcome Trust (FC001076). E-MF was supported by a Wellcome Trust Career Development Fellowship (091664/B/10/Z).

SUPPLEMENTARY MATERIAL

The Supplementary Material for this article can be found online at https://www.frontiersin.org/articles/10.3389/fimmu.2018.01290/full#supplementary-material.

REFERENCES

1. Joshi NS, Cui W, Chandele A, Lee HK, Urso DR, Hagman J, et al. Inflammation directs memory precursor and short-lived effector CD8+ T cell fates via the graded expression of T-bet transcription factor. *Immunity* (2007) 27:281–95. doi:10.1016/j.immuni.2007.07.010
2. Zehn D, Lee SY, Bevan MJ. Complete but curtailed T-cell response to very low-affinity antigen. *Nature* (2009) 458:211–4. doi:10.1038/nature07657
3. Virgin HW, Wherry EJ, Ahmed R. Redefining chronic viral infection. *Cell* (2009) 138:30–50. doi:10.1016/j.cell.2009.06.036
4. Wherry EJ. T cell exhaustion. *Nat Immunol* (2011) 12:492–9. doi:10.1038/ni.2035
5. Merkenschlager J, Kassiotis G. Narrowing the gap: preserving repertoire diversity despite clonal selection during the CD4 T cell response. *Front Immunol* (2015) 6:413. doi:10.3389/fimmu.2015.00413
6. Mandl JN, Monteiro JP, Vrisekoop N, Germain RN. T cell-positive selection uses self-ligand binding strength to optimize repertoire recognition of foreign antigens. *Immunity* (2013) 38:263–74. doi:10.1016/j.immuni.2012.09.011
7. Parker SJ, Roberts CW, Alexander J. CD8+ T cells are the major lymphocyte subpopulation involved in the protective immune response to *Toxoplasma gondii* in mice. *Clin Exp Immunol* (1991) 84:207–12. doi:10.1111/j.1365-2249.1991.tb08150.x
8. Suzuki Y, Conley FK, Remington JS. Importance of endogenous IFN-gamma for prevention of toxoplasmic encephalitis in mice. *J Immunol* (1989) 143:2045–50.
9. Brown CR, Mcleod R. Class I MHC genes and CD8+ T cells determine cyst number in *Toxoplasma gondii*. *J Immunol* (1990) 145:3438–41.
10. Brown CR, Hunter CA, Estes RG, Beckmann E, Forman J, David C, et al. Definitive identification of a gene that confers resistance against *Toxoplasma* cyst burden and encephalitis. *Immunology* (1995) 85:419–28.
11. Blanchard N, Gonzalez F, Schaeffer M, Joncker NT, Cheng T, Shastri AJ, et al. Immunodominant, protective response to the parasite *Toxoplasma gondii* requires antigen processing in the endoplasmic reticulum. *Nat Immunol* (2008) 9:937–44. doi:10.1038/ni.1629
12. Suzuki Y, Joh K, Orellana MA, Conley FK, Remington JS. A gene(s) within the H-2D region determines the development of toxoplasmic encephalitis in mice. *Immunology* (1991) 74:732–9.
13. Suzuki Y, Sa Q, Gehman M, Ochiai E. Interferon-gamma- and perforin-mediated immune responses for resistance against *Toxoplasma gondii* in the brain. *Expert Rev Mol Med* (2011) 13:e31. doi:10.1017/S1462399411002018
14. Chu HH, Chan SW, Gosling JP, Blanchard N, Tsitsiklis A, Lythe G, et al. Continuous effector CD8+ T cell production in a controlled persistent infection is sustained by a proliferative intermediate population. *Immunity* (2016) 45:159–71. doi:10.1016/j.immuni.2016.06.013
15. Wakim LM, Woodward-Davis A, Liu R, Hu Y, Villadangos J, Smyth G, et al. The molecular signature of tissue resident memory CD8 T cells isolated from the brain. *J Immunol* (2012) 189:3462–71. doi:10.4049/jimmunol.1201305
16. Schenkel JM, Fraser KA, Masopust D. Cutting edge: resident memory CD8 T cells occupy frontline niches in secondary lymphoid organs. *J Immunol* (2014) 192:2961–4. doi:10.4049/jimmunol.1400003
17. Gebhardt T, Mackay LK. Local immunity by tissue-resident CD8+ memory T cells. *Front Immunol* (2012) 3:340. doi:10.3389/fimmu.2012.00340
18. Mackay LK, Stock AT, Ma JZ, Jones CM, Kent SJ, Mueller SN, et al. Long-lived epithelial immunity by tissue-resident memory T (TRM) cells in the absence of persisting local antigen presentation. *Proc Natl Acad Sci U S A* (2012) 109:7037–42. doi:10.1073/pnas.1202288109
19. Sheridan BS, Pham QM, Lee YT, Cauley LS, Puddington L, Lefrançois L. Oral infection drives a distinct population of intestinal resident memory CD8+ T cells with enhanced protective function. *Immunity* (2014) 40:747–57. doi:10.1016/j.immuni.2014.03.007
20. Wakim LM, Woodward-Davis A, Bevan MJ. Memory T cells persisting within the brain after local infection show functional adaptations to their tissue of residence. *Proc Natl Acad Sci U S A* (2010) 107:17872–9. doi:10.1073/pnas.1010201107
21. Ariotti S, Beltman JB, Chodaczek G, Hoekstra ME, van Beek AE, Gomez-Eerland R, et al. Tissue-resident memory CD8+ T cells continuously patrol skin epithelia to quickly recognize local antigen. *Proc Natl Acad Sci U S A* (2012) 109:19739–44. doi:10.1073/pnas.1208927109

22. Steinert EM, Schenkel JM, Fraser KA, Beura LK, Manlove LS, Igyártó BZ, et al. Quantifying memory CD8 T cells reveals regionalization of immunosurveillance. *Cell* (2015) 161:737–49. doi:10.1016/j.cell.2015.03.031
23. Landrith TA, Sureshchandra S, Rivera A, Jang JC, Rais M, Nair MG, et al. CD103+ CD8 T cells in the *Toxoplasma*-infected brain exhibit a tissue-resident memory transcriptional profile. *Front Immunol* (2017) 8:335. doi:10.3389/fimmu.2017.00335
24. Kirak O, Frickel EM, Grotenbreg GM, Suh H, Jaenisch R, Ploegh HL. Transnuclear mice with predefined T cell receptor specificities against *Toxoplasma gondii* obtained via SCNT. *Science* (2010) 328:243–8. doi:10.1126/science.1178590
25. Swee LK, Tan ZW, Sanecka A, Yoshida N, Patel H, Grotenbreg G, et al. Peripheral self-reactivity regulates antigen-specific CD8 T-cell responses and cell division under physiological conditions. *Open Biol* (2016) 6:160293. doi:10.1098/rsob.160293
26. Pino PA, Cardona AE. Isolation of brain and spinal cord mononuclear cells using Percoll gradients. *J Vis Exp* (2011) 48:2348. doi:10.3791/2348
27. Martinez RJ, Andargachew R, Martinez HA, Evavold BD. Low-affinity CD4+ T cells are major responders in the primary immune response. *Nat Commun* (2016) 7:1–10. doi:10.1038/ncomms13848
28. Merkenschlager J, Ploquin MJ, Eksmond U, Andargachew R, Thorborn G, Filby A, et al. Stepwise B-cell-dependent expansion of T helper clonotypes diversifies the T-cell response. *Nat Commun* (2016) 7:10281. doi:10.1038/ncomms10281
29. Frickel E, Sahoo N, Hopp J, Gubbels M, Craver MPJ, Knoll LJ, et al. Parasite stage-specific recognition of endogenous *Toxoplasma gondii*-derived CD8 $^{+}$ T cell epitopes. *J Infect Dis* (2008) 198:1625–33. doi:10.1086/593019
30. Li B, Dewey CN. RSEM: accurate transcript quantification from RNA-seq data with or without a reference genome. *BMC Bioinformatics* (2011) 12:323. doi:10.1186/1471-2105-12-323
31. Karolchik D, Hinrichs AS, Furey TS, Roskin KM, Sugnet CW, Haussler D, et al. The UCSC table browser data retrieval tool. *Nucleic Acids Res* (2004) 32:D493–6. doi:10.1093/nar/gkh103
32. Love MI, Huber W, Anders S. Moderated estimation of fold change and dispersion for RNA-seq data with DESeq2. *Genome Biol* (2014) 15:1–21. doi:10.1186/s13059-014-0550-8
33. Frost EL, Kersh AE, Evavold BD, Lukacher AE. Cutting edge: resident memory CD8 T cells express high-affinity TCRs. *J Immunol* (2015) 195:3520–4. doi:10.4049/jimmunol.1501521
34. Hood JD, Zarnitsyna VI, Zhu C, Evavold BD. Regulatory and T effector cells have overlapping low to high ranges in TCR affinities for self during demyelinating disease. *J Immunol* (2015) 195:4162–70. doi:10.4049/jimmunol.1501464
35. Weinreich MA, Takada K, Skon C, Reiner SL, Jameson SC, Hogquist KA. KLF2 transcription-factor deficiency in T cells results in unrestrained cytokine production and upregulation of bystander chemokine receptors. *Immunity* (2009) 31:122–30. doi:10.1016/j.immuni.2009.05.011
36. Carlson CM, Endrizzi BT, Wu J, Ding X, Weinreich MA, Walsh ER, et al. Kruppel-like factor 2 regulates thymocyte and T-cell migration. *Nature* (2006) 442:299–302. doi:10.1038/nature04882
37. Bai A, Hu H, Yeung M, Chen J. Kruppel-like factor 2 controls T cell trafficking by activating L-selectin (CD62L) and sphingosine-1-phosphate receptor 1 transcription. *J Immunol* (2007) 178:7632–9. doi:10.4049/jimmunol.178.12.7632
38. Schober SL, Kuo CT, Schluns KS, Lefrancois L, Leiden JM, Jameson SC. Expression of the transcription factor lung Krüppel-like factor is regulated by cytokines and correlates with survival of memory T cells in vitro and in vivo. *J Immunol* (1999) 163:3662–7.
39. Preston GC, Feijoo-Carnero C, Schurch N, Cowling VH, Cantrell DA. The impact of KLF2 modulation on the transcriptional program and function of CD8 T cells. *PLoS One* (2013) 8:e77537. doi:10.1371/journal.pone.0077537
40. Zehn D, Utzschneider DT, Thimme R. Immune-surveillance through exhausted effector T-cells. *Curr Opin Virol* (2016) 16:49–54. doi:10.1016/j.coviro.2016.01.002
41. Wilson EH, Harris TH, Mrass P, John B, Tait ED, Wu GF, et al. Behavior of parasite-specific effector CD8+ T cells in the brain and visualization of a kinesis-associated system of reticular fibers. *Immunity* (2009) 30:300–11. doi:10.1016/j.immuni.2008.12.013
42. Bhadra R, Gigley JP, Weiss LM, Khan IA. Control of *Toxoplasma* reactivation by rescue of dysfunctional CD8+ T-cell response via PD-1-PDL-1 blockade. *Proc Natl Acad Sci U S A* (2011) 108:9196–201. doi:10.1073/pnas.1015298108
43. Wherry EJ, Kurachi M. Molecular and cellular insights into T cell exhaustion. *Nat Rev Immunol* (2015) 15:486–99. doi:10.1038/nri3862
44. Zhang B, Chan YK, Lu B, Diamond MS, Klein RS. CXCR3 mediates region-specific antiviral T cell trafficking within the central nervous system during West Nile virus encephalitis. *J Immunol* (2008) 180:2641–9. doi:10.4049/jimmunol.180.4.2641
45. Hogan T, Gossel G, Yates AJ, Seddon B. Temporal fate mapping reveals age-linked heterogeneity in naive T lymphocytes in mice. *Proc Natl Acad Sci U S A* (2015) 112:E6917–26. doi:10.1073/pnas.1517246112
46. King CG, Koehli S, Hausmann B, Schmaler M, Zehn D, Palmer E. T cell affinity regulates asymmetric division, effector cell differentiation, and tissue pathology. *Immunity* (2012) 37:709–20. doi:10.1016/j.immuni.2012.06.021
47. Man K, Miasari M, Shi W, Xin A, Henstridge DC, Preston S, et al. The transcription factor IRF4 is essential for TCR affinity-mediated metabolic programming and clonal expansion of T cells. *Nat Immunol* (2013) 14:1155–65. doi:10.1038/ni.2710
48. Krummel MF, Allison JP. CD28 and CTLA-4 have opposing effects on the response of T cells to stimulation. *J Exp Med* (1995) 182:459–65. doi:10.1084/jem.182.2.459
49. Greenwald RJ, Boussiotis VA, Lorsbach RB, Abbas AK, Sharpe AH. CTLA-4 regulates induction of anergy in vivo. *Immunity* (2001) 14:145–55. doi:10.1016/S1074-7613(01)00097-8
50. Jain N, Miu B, Jiang J, McKinstry KK, Prince A, Swain SL, et al. CD28 and ITK signals regulate autoreactive T cell trafficking. *Nat Med* (2013) 19:1632–7. doi:10.1038/nm.3393
51. Gibson HM, Hedgcock CJ, Aufiero BM, Wilson AJ, Hafner MS, Tsokos GC, et al. Induction of the CTLA-4 gene in human lymphocytes is dependent on NFAT binding the proximal promoter. *J Immunol* (2007) 179:3831–40. doi:10.4049/jimmunol.179.6.3831
52. Vezys V, Masopust D, Kemball CC, Barber DL, O'Mara LA, Larsen CP, et al. Continuous recruitment of naive T cells contributes to heterogeneity of antiviral CD8 T cells during persistent infection. *J Exp Med* (2006) 203:2263–9. doi:10.1084/jem.20060995
53. Gebhardt T, Wakim LM, Eidsmo L, Reading PC, Heath WR, Carbone FR. Memory T cells in nonlymphoid tissue that provide enhanced local immunity during infection with herpes simplex virus. *Nat Immunol* (2009) 10:524–30. doi:10.1038/ni.1718
54. Skon CN, Lee JY, Anderson KG, Masopust D, Hogquist KA, Jameson SC. Transcriptional downregulation of S1pr1 is required for the establishment of resident memory CD8+ T cells. *Nat Immunol* (2013) 14:1285–93. doi:10.1038/ni.2745
55. Casey KA, Fraser KA, Schenkel JM, Moran A, Abt MC, Beura LK, et al. Antigen-independent differentiation and maintenance of effector-like resident memory T cells in tissues. *J Immunol* (2012) 188:4866–75. doi:10.4049/jimmunol.1200402
56. Masopust D, Choo D, Vezys V, Wherry EJ, Duraiswamy J, Akondy R, et al. Dynamic T cell migration program provides resident memory within intestinal epithelium. *J Exp Med* (2010) 207:553–64. doi:10.1084/jem.20090858
57. Beura LK, Anderson KG, Schenkel JM, Locquiao JJ, Fraser KA, Vezys V, et al. Lymphocytic choriomeningitis virus persistence promotes effector-like memory differentiation and enhances mucosal T cell distribution. *J Leukoc Biol* (2015) 97:217–25. doi:10.1189/jlb.1HI0314-154R
58. Fulton RB, Hamilton SE, Xing Y, Best JA, Goldrath AW, Hogquist KA, et al. The TCR's sensitivity to self peptide-MHC dictates the ability of naive CD8+ T cells to respond to foreign antigens. *Nat Immunol* (2015) 16:107–17. doi:10.1038/ni.3043
59. Zajac AJ, Blattman JN, Murali-Krishna K, Sourdive DJD, Suresh M, Altman JD, et al. Viral immune evasion due to persistence of activated T cells without effector function. *J Exp Med* (1998) 188:2205–13. doi:10.1084/jem.188.12.2205
60. Wherry EJ, Blattman JN, Murali-krishna K, Van Der Most R, Ahmed R. Viral persistence alters CD8 T-cell immunodominance and tissue distribution and results in distinct stages of functional impairment viral persistence alters CD8 T-cell immunodominance and tissue distribution and results in distinct stages of functional impairment. *J Virol* (2003) 77:4911–27. doi:10.1128/JVI.77.8.4911

61. Bhadra R, Khan IA. IL-7 and IL-15 do not synergize during CD8 T cell recall response against an obligate intracellular parasite. *Microbes Infect* (2012) 14:1160–8. doi:10.1016/j.micinf.2012.07.018

Conflict of Interest Statement: The authors declare that the research was conducted in the absence of any commercial or financial relationships that could be construed as a potential conflict of interest.